International Journal of Mass Spectrometry 280 (2009) 169–173

Contents lists available at ScienceDirect

International Journal of Mass Spectrometry

journal homepage: www.elsevier.com/locate/ijms

Electron impact ionisation and UV absorption study of α- and β-pinene

D. Kubala[a], E.A. Drage[b], A.M.E. Al-Faydhi[c], J. Kočíšek[a], P. Papp[a], V. Matejčík[d], P. Mach[e], J. Urban[d], P. Limão-Vieira[b,f], S.V. Hoffmann[g], Š. Matejčík[a,*], N.J. Mason[b]

[a] Department of Experimental Physics, Comenius University, Mlynská dolina F2, 84248 Bratislava, Slovakia
[b] Department of Physics and Astronomy, The Open University, Walton Hall, Milton Keynes MK7 6AA, United Kingdom
[c] Department of Physics, College of Science, Mosul University, Mosul, Iraq
[d] Faculty of Medicine, Comenius University, Špitálska 24, 813 72 Bratislava, Slovakia
[e] Department of Nuclear Physics and Biophysics, Comenius University, Mlynská dolina F2, 84248 Bratislava, Slovakia
[f] Atomic and Molecular Collisions Laboratory, CEFITEC, Departamento de Física, Universidade Nova de Lisboa, 2829-516 Caparica, Portugal
[g] Institute for Storage Ring Facilities, University of Aarhus, Ny Munkegade, DK-8000 Arhus C, Denmark

ARTICLE INFO

Article history:
Received 25 June 2008
Received in revised form 27 July 2008
Accepted 31 July 2008
Available online 8 August 2008

Keywords:
α-Pinene
β-Pinene
VUV photoabsorption
Electron impact ionisation

ABSTRACT

We have performed a coordinated set of experiments to measure the electron impact ionisation and UV photoabsorption cross sections of α- and β-pinene. The adiabatic ionisation energies of α- and β-pinene were derived from experiment and found to be 8.3 and 8.6 eV which compared well with high-level quantum chemical calculations (G3MP2) yielding values of 8.29 and 8.41 eV. Additionally, vertical ionisation energies of 8.62 and 8.96 eV were calculated using an OVGF method. UV photoabsorption cross sections were measured using a high-resolution synchrotron radiation source and electronic states interpreted on the basis of the TD quantum chemical methods.

1. Introduction

Chemical processes occurring in the troposphere have a direct impact on both global and local climatic changes. Such processes are strongly influenced by the presence of volatile organic compounds (VOCs) [1,2]. Recent research shows that the amount of naturally produced VOCs exceeds anthropogenic sources by several orders of magnitude [3,4]. The most abundant naturally formed VOCs are isoprenes and isoprene chains called monoterpenes, the latter making up more than half (54%) of total natural VOCs production [5].

Monoterpenes are also the precursor for creation of many terrestrial secondary organic aerosols (SOAs) formed by a series of gas-to-particle chemical reactions from natural VOCs [6], however many of these reactions remain unquantified. SOAs affect radiation balance both directly by scattering and/or absorbing sunlight [7–9] and indirectly as cloud condensation nuclei. α-Pinene (35%) and β-pinene (23%) are the most abundant monoterpenes in the Earth's atmosphere [3]. Nevertheless many of their basic properties such as ionisation cross sections, the appearance energies (AEs) of fragment ions and UV transmission spectra of both α- and β-pinene are still missing or are somewhat old and need to be reviewed [10,11].

In this paper, we report the results of a new set of experiments to explore the electronic state spectroscopy and ionisation of α- and β-pinene. High-resolution UV absorption spectra of both compounds have been measured using synchrotron radiation. The present data have both a higher resolution and increased sensitivity compared to the only set of earlier data [12]. In order to interpret the UV spectra and assign electronic excited states of the molecules to observed spectral bands we have also performed quantum chemical calculations to classify valence and Rydberg states that may contribute to the absorption bands.

In order to explore Rydberg states of these molecules it is necessary to determine the ionisation energies (EIs) of the molecules. We have studied two electron impact ionisation (EII) processes:

$$e + M \rightarrow M^+ + 2e \quad \text{(direct ionisation)} \tag{1}$$

and

$$e + M \rightarrow X^+ + M\text{–}X + 2e \quad \text{(dissociative ionisation)} \tag{2}$$

of gas phase α- and β-pinene. We have measured the IEs and the AEs of ionic fragments. The values of the vertical ionisation energies derived from these experiments are compared with

* Corresponding author.
E-mail address: matejcik@fmph.uniba.sk (Š. Matejčík).

1387-3806/$ – see front matter © 2008 Elsevier B.V. All rights reserved.
doi:10.1016/j.ijms.2008.07.035

values we have calculated using standard quantum chemical methods.

To our knowledge, this is the first EII study of α- and β-pinene, however, there is an earlier HeI photoelectron spectroscopy (PES) study by Novak and Kovac [12] of three natural monoterpenes – pinene, pulegone and cembrene – with which we can compare our derived ionisation energies. Novak and Kovac also performed Hartree–Fock and density functional theory calculations for the orbital energy of the outgoing electron, their derived value of 8.27 eV being in good agreement with the experimentally derived vertical ionisation energy (E_i = 8.38 eV) for α-pinene. In their PES spectrum of α-pinene, the band at 8.38 eV was assigned to the single, endocyclic π-orbital. Ionisation potentials (IPs) lower than 21.21 eV were derived from the photoelectron spectra of 48 organic compounds by Al-Joboury and Turner [11] in 1964, for α-pinene an ionisation energy of E_i = 8.07 eV was estimated. A mass spectrometric study of α-pinene produced by electron impact dissociative ionisation of α-pinene was published by Mormann et al. [16] using a Fourier transform-ion cyclotron resonance (FT-ICR) spectrometer. Only ions with the mass to charge ratio m/z = 93 ($C_7H_9^+$) were detected. According to this study about 85% of the most abundant ion $C_7H_9^+$ consists of protonated toluene molecule—toluenium. Unfortunately no similar study was performed for the isomer β-pinene.

2. Experimental apparatus and computational methods

Two sets of experiments were performed on α- and β-pinene: (i) VUV spectroscopy and (ii) electron impact studies. The liquid samples were purchased from Sigma–Aldrich with a stated purity of 98%. The sample was degassed by a repeated freeze-pump-thaw cycle.

2.1. UV spectroscopy

High-resolution vacuum ultraviolet photoabsorption spectra of α- and β-pinene were recorded using synchrotron radiation on the ultraviolet vacuum line (UV1) of the ASTRID facility at University Aarhus, Denmark. The apparatus has been described in detail elsewhere [30], so only a brief description is given here.

The apparatus consists of a static gas cell with an absorption path length of 25 cm. A photomultiplier tube recorded the transmitted light intensity, I_t, exiting the gas filled cell, at 0.05 nm intervals. The sample pressure was measured at each wavelength using an MKS 390HA Baratron Capacitance Manometer, accuracy ±0.1%. These results were compared with a transmission spectrum recorded with the cell evacuated, I_0. The absolute photoabsorption cross section was then determined using the Beer–Lambert law:

$$I_t = I_0 \exp(-n\sigma x) \quad (3)$$

where n is the target gas number density, σ is the absorption cross section and x is the path length of the gas cell. The synchrotron ring beam current was monitored continuously as a monitor of the any changes in the incident UV flux.

Spectra were recorded between 10.8 and 3.9 eV (115 and 320 nm) with a typical resolution of 0.075 nm, at FWHM. The minimum and maximum wavelengths are determined by the cell window transmission cut-off and the grating range, respectively. Cross sections were measured over a range of pressures (0.01–0.8 mbar) to ensure that any data collected was free of any saturation effects (typical attenuation <10%). For wavelengths below 6.20 eV (200 nm), helium was flushed through the small gap between the photomultiplier and the exit window of the gas cell to prevent any absorption by air contributing to the spectrum. At longer wavelengths, absorption by the air in the gap removes the higher-order radiation.

2.2. Electron impact ionisation

Electron impact ionisation data were collected using the crossed electron/molecular beam apparatus at Bratislava laboratory. The apparatus has been described in detail previously [13], thus only a brief description is given here.

The electron beam was formed in a trochoidal electron monochromator (TEM) with an electron energy resolution of about 140 meV. The electron energy scale was calibrated by measuring the Ar^+ ion efficiency curve for the reaction:

$$e^- + Ar \rightarrow Ar^+ + 2e^- \quad (4)$$

that has an established ionisation energy of 15.759 ± 0.001 eV [14]. The molecular beam was produced in a temperature controlled effusive molecular beam source (EMBS). The beam was formed via effusion through a capillary (0.5 mm diameter and 4 mm long).

The ions formed in the interaction between the electron and the molecular beams were extracted by a weak electric field into a quadrupole mass spectrometer (QMS). Ion yields thus were recorded as a function of the electron energy. It was necessary to accumulate data over very long time periods in order to achieve high sensitivity and accuracy and to detect reactions with very low cross sections. The stability of the experimental conditions during these long data collection periods (e.g., drift of the power supplies) was checked by the measurement of reaction (4) at the beginning and the end of the experiment. The stability was typically about 10 meV/day.

The measured ionisation efficiency curves were analyzed using a well-established data analysis methodology [15]. This method takes into account the finite width of the kinetic energy distribution function of the electrons in the electron beam and enables appearance energies of ions produced by dissociative electron ionisation to be determined with very high accuracy (±20 meV).

2.3. Computational methods

The standard G3MP2 methodology [16] was used for the calculation of reaction enthalpies of the fragmentation reactions (at 298.15 K and 101.325 kPa) and for calculation of the adiabatic ionisation energies of α- and β-pinene. A similar methodology was also used for calculating vertical IPs (at geometries of neutral species optimized using B3LYP/6-311+G(2d,2p) level of theory). All calculations were made using the MULTILEVEL4.0 [17] and GAUSSIAN03 [18] programmes. Excitation energies and oscillator strengths for VUV spectra of α- and β-pinene were calculated using Configuration Interaction with Single replacement from reference configurations (CIS) [19], and CIS with correction for double replacement from reference configuration—CIS(D) [20] and time-dependent DFT (TDDFT) theory [21] as implemented in the GAUSSIAN03 and PC-GAMESS [22] computer codes. In all these calculations the frozen core option was used, i.e., excitations from the 1s orbitals of constituent carbon atoms were excluded. Spectral calculations were performed using a geometry of neutral molecule, optimized at B3LYP/6-311+G(2d,2p). As excited states have, in general, a more diffuse character than ground state, for excited state calculations some diffuse functions should be included. Calculations at CIS(D) level were therefore performed using 6-31(2+)+G** basis set (standard 6-31++G** set [22] augmented with an extra p shell on the carbon atoms with an exponent of 0.0131928) [23], TDDFT calculations were made with 6-311(2+)+G** basis, defined as above.

3. Results and discussion

3.1. Electron impact ionisation

Electron impact generally results in intense fragmentation of the target molecule, especially in the case of large molecules such as α- and β-pinene. The product mass spectra were recorded at an incident electron energy of 70 eV (Fig. 1). The recorded spectra are broadly consistent with the data recorded in the US National Institute of Standards and Technology (NIST) database [14]. The main difference in the present mass spectra of these two molecules is the presence of an ion with $m/z = 69$ in the mass spectra of β-pinene which is totally absent in the mass spectra of α-pinene. Thus, this ion may be used as a marker for β-pinene molecules. This difference is most probably due to the position of the carbon–carbon double bond in the naturally less abundant isomer β-pinene. Stoichiometric identification of the ions with given m/z in pinenes is relatively easy due to the fact, that they are formed only from carbon and hydrogen atoms.

We have measured the ionisation efficiency curves for the 13 most abundant fragment ions and derived their appearance energies (see Table 1). For the majority of the fragments we observe a difference in the appearance energies of the ions emerging from α- and β-pinene (an isomeric effect) of about 0.3 eV. This difference is significantly larger than the evaluated error bars arising from the experimental method and fitting technique (typically 20–100 meV).

Such mass spectrometric measurements provide little information on the structure of the fragment cations. Therefore, using G3MP2 methodology we calculated the structures and energies of the neutral molecules and radicals of several positive ions. The ionic conformations with the lowest energy are considered to be the most stable and are the most likely structures of individual ions formed by electron impact close to threshold. Present calculations indicate that the α-pinene cation maintains its parent's ring structure, whereas the β-pinene cation is formed through opening the ring.

Table 1
Appearance energies (AEs) for fragment cations produced by electron impact ionisation of α- and β-pinene

Mass (amu)	AE (eV)		Formula
	α-Pinene	β-Pinene	
27	15.04 ± 0.27	17.39 ± 0.30	$C_2H_3^+$
39	16.85 ± 0.24	15.50 ± 0.30	$C_3H_3^+$
41	13.62 ± 0.10	13.34 ± 0.05	$C_3H_5^+$
53	14.59 ± 0.10	14.59 ± 0.10	$C_4H_5^+$
67	12.01 ± 0.09	11.16 ± 0.20	$C_5H_7^+$
69	Missing ion	11.17 ± 0.04	$C_5H_9^+$
77	12.45 ± 0.05	12.49 ± 0.05	$C_6H_5^+$
79	10.90 ± 0.05	10.48 ± 0.05	$C_6H_7^+$ (protonated benzene)
91	12.38 ± 0.05	12.17 ± 0.05	$C_7H_7^+$ (benzyl cation)
93	8.97 ± 0.04	9.13 ± 0.04	$(M\text{-}C_3H_7)^+$
105	12.64 ± 0.05	13.03 ± 0.08	$(M\text{-}C_2H_6)^+ + C_2H_6 + H$ (methyl benzyl cation)
107	10.19 ± 0.11	10.22 ± 0.06	$(M\text{-}C_2H_5)^+ + C_2H_5$
121	9.81 ± 0.05	9.99 ± 0.04	$(M\text{-}CH_3)^+ + CH_3$ (protonated mesitylene)
136	8.30 ± 0.02	8.60 ± 0.03	M^+

The ionisation efficiency curves of the parent molecular ions are presented in Fig. 2. Our derived experimental value for the ionisation energy of α-pinene (8.30 ± 0.02 eV) is in excellent agreement with the PES results of Novak and Kovac [12], 8.38 eV. We are not aware of any earlier measurements of the ionisation energy of β-pinene which we evaluate to be 8.60 ± 0.03 eV. The ionisation efficiency curves of both α- and β-pinene provide evidence for an additional threshold at 8.54 and 8.98 eV, respectively. These we associate with an additional ionic state of the pinene cations.

Present calculations at G3MP2 level give adiabatic ionisation energies of 8.29 eV for α-pinene and 8.42 eV for β-pinene. The values calculated at B3LYP/6-311+G(2df,2p) level give values of 7.81 and 7.83 eV, respectively. According to Ref. [24], average absolute deviation of IE is for G3MP2 0.08 eV and for B3LYP 0.18 eV. The G3MP2 method generally shows fewer outlying results than B3LYP so we believe that the real value is close to the G3MP2 value, which is in good agreement with the measured appearance ener-

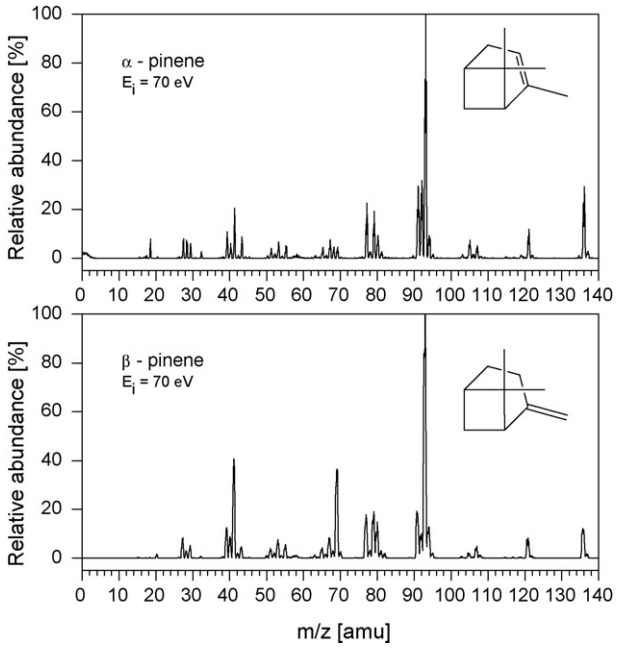

Fig. 1. Mass spectrum of α- and β-pinene recorded at an incident electron energy of 70 eV.

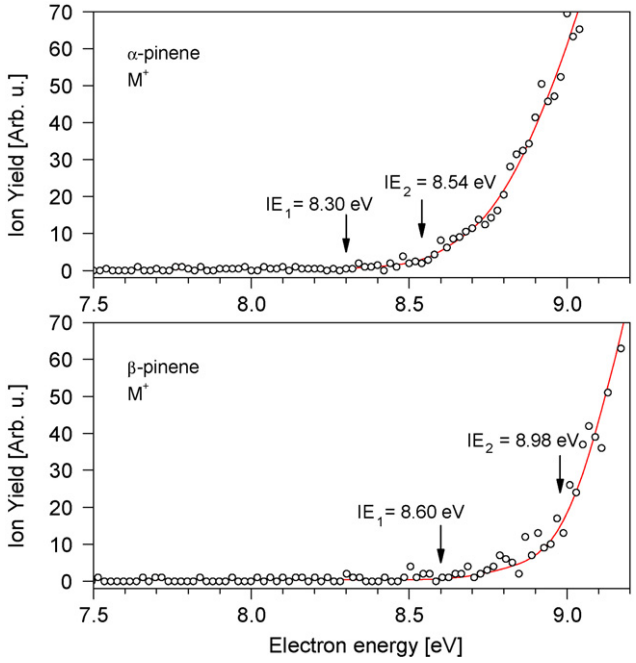

Fig. 2. Threshold ionisation yields for α- and β-pinene parent cations.

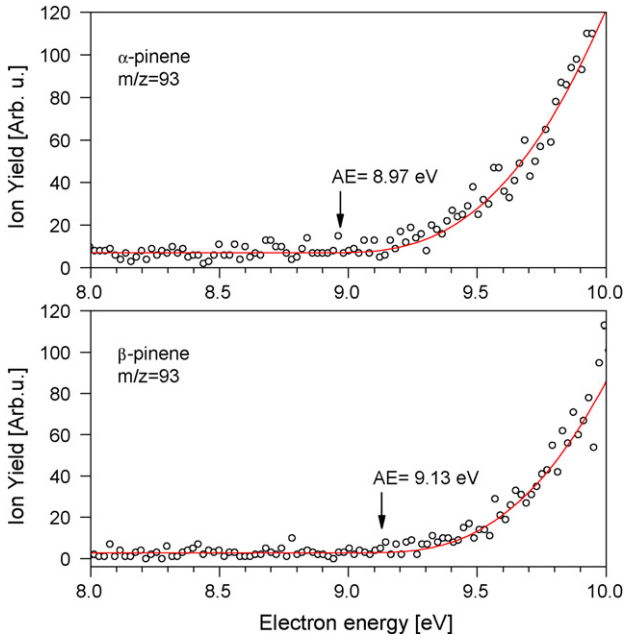

Fig. 3. Threshold ionisation yields for cationic fragments of $m/z = 93$ produced by electron impact of α- and β-pinene.

gies 8.30 and 8.60 eV. We have estimated vertical IE at G3MP2 level (i.e., difference of total energies as defined in G3MP2 methodology, excluding vibrational contribution, calculated both for the neutral molecule and the cation in the B3LYP/6-311+G(2d,2p) optimized geometry of the neutral molecule) of 8.62 and 8.96 eV for α- and β-pinene, respectively. Vertical IEs can also be calculated using an OVGF methodology [25]. These calculations, using 6-311+G(2df,2p) basis and the above-mentioned geometry of neutral molecule provide IEs of 8.57 and 8.90 eV for α- and β-pinene, respectively.

Dissociation following electron impact ionisation of α- and β-pinene results in the formation of large number of ions. The list of the appearance energies for all measured ions is presented in Table 1 for both isomers. For the majority of the ions there exist only small differences (0–0.5 eV) in the appearance energies of the ions from α- and β-pinene. However, pronounced differences in the two isomers are observed for small fragment ions with $m/z = 27$, 39 (more than 1 eV) and 67 (about 1 eV). Furthermore ions with a $m/z = 69$ were produced from β-pinene but were not observed in the mass spectrum of α-pinene. The absence of this ion in the α-pinene spectrum is most probably due to the stabilising effect of the π-bond on the cyclic structure in the α-pinene molecule, as the cation $m/z = 69$ can only be formed via dissociation of the cyclic structure. According to Cecchi et al. [26], it is the largest ion formed from pinenes with open conformation.

Ion yield curves for formation of the most abundant fragment ions with $m/z = 93$ ($C_7H_9^+$) are presented in Fig. 3. This ion is very stable and most probably has a form of protonated toluene [14]. However, to confirm this by calculations we would need some information about the neutral fragments formed in this reaction.

3.2. UV spectra

The UV absorption spectra of α- and β-pinene are shown in Fig. 4. The spectra were measured over the photon energy range of 5.5–10.7 eV. Below the ionisation energy the UV spectra show broad structures. Above 7 eV we see a monotonic increase in the absorption cross section which is most probably associated with dissociation from valence electronic states. The spectra from the

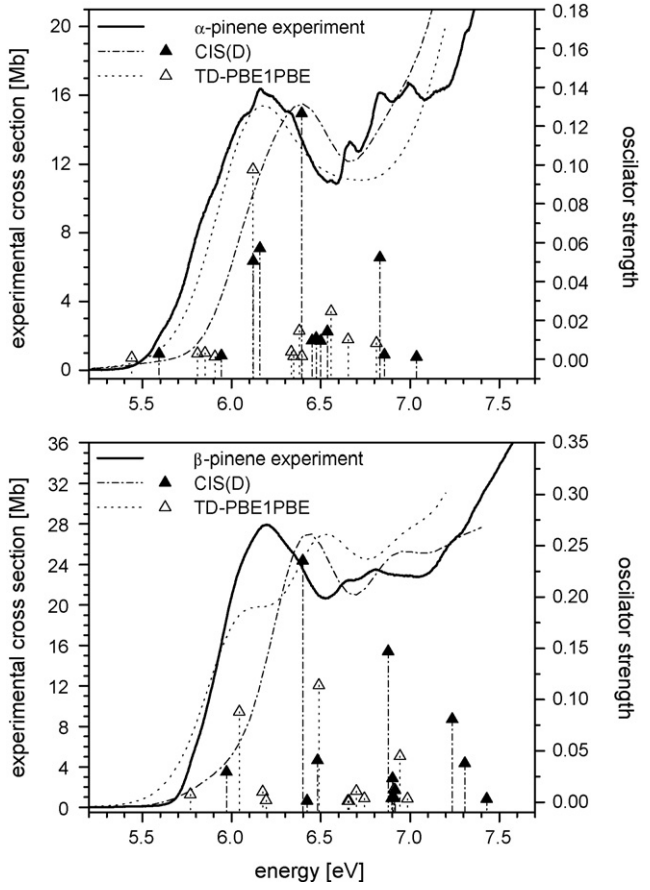

Fig. 4. VUV spectrum of α- and β-pinene compared with electronic state thresholds derived using CIS(D) and TDDFT calculations (see text for details).

two isomers are therefore similar but the fine structure is clearly much sharper in the α-pinene spectrum with three distinct peaks being observed above 6.5 eV in α-pinene whilst these peaks are very diffuse in β-pinene. The onset (excitation energy) in α-pinene is noticeably lower than that in β-pinene as is the cross section.

In order to assign observed band features with the valence and Rydberg states we have performed CI calculations of the excited states of both the α- and β-pinene. The first peak in the UV absorption spectra we associate with π–π^* transitions since the electronic state with strongest oscillator strength has a π^* character. However, several additional weaker transitions to other virtual orbitals were calculated in the 5–7 eV range and may account for the fine structure observed around the maximum in the α-pinene spectrum.

Although rigorous theoretical interpretation of UV spectra of molecules as large as pinene are still quite expensive tasks, we can try to reproduce the few lowest-energy transitions using both CIS(D) and TDDFT methods. Both these methods are known to give semi-quantitative agreement for transition energies for excited states that are primarily one-electron transitions. Fig. 4 shows the first 12 transitions as calculated at CIS(D)/6-31(2+)+G** and TDDFT/6-311(2+)+G** level using PBE1PBE hybrid density functional [27]. Calculated transitions are convoluted with Gaussian functions of 0.2 eV half-widths to simulate vibrational broadening. To simulate the effect of higher excitations, which are responsible for the steady increase in the cross section beyond the first peak, one extra Gaussian centred at 11 eV and very high intensity ($\sim f = 18$) was added to these pictures. In Fig. 4, we can see that both CIS(D) and TDDFT calculations replicate the relative shift in the first peak of α-pinene towards lower energies and lower intensities, relative to

β-pinene. CIS(D) transition energies are systematically higher (by about 0.2 eV) compared to experiment. TDDFT on the other hand gives a relatively good description of first peak for α-pinene, but the agreement is not so good in the case of β-pinene. This may be generally ascribed to the poor asymptotic behaviour of most of the currently used approximate density functionals. Casida et al. [28] and Tozer and Handy [29] have shown that the excitation energy of valence states are relatively well described by TDDFT, but excitations with significant Rydberg character are systematically underestimated. A rough but useful criterion for discriminating between the two types of excitation is the energy of the highest occupied Kohn–Shamm orbital. Excitations below the ionisation threshold ($\sim -\varepsilon_{HOMO}$) are valence; above the ionisation threshold they have Rydberg character. Unfortunately in both α- and β-pinene only the first peak lies below the ionisation threshold and Rydberg excitations will be integral to the recorded UV spectrum.

4. Conclusions

We report the first coordinated experimental study of the electron impact ionisation and the UV absorption cross sections of two of the most abundant monoterpenes: α- and β-pinene.

We have measured the electron impact ionisation mass spectra of both isomers at the standard electron impact energy of 70 eV and measured the ion yield curves of the 13 most intense ions from the mass spectrum of α-pinene and 14 peaks from the spectrum of β-pinene. From these ionisation curves we have derived the appearance energies of each fragment ion. Some significant differences were observed between the two isomers which could be used to separately detect these compounds in the terrestrial atmosphere, in particular ions with a $m/z = 69$ were produced from β-pinene but were not observed in the mass spectrum from α-pinene molecule.

Acknowledgements

This work was financially supported by the UK NERC Research Agency and the Slovak Science and Technology Assistance Agency under the contract no. APVT-20-007504, and VEGA Grant Agency, Slovakia, under the project no. 1/3040/06. One of us (EAD) acknowledges receipt of a UK NERC Postgraduate studentship and support of Anglo Danish Society and CN Davies Award of the UK Aerosol Society. The authors also wish to acknowledge beam time granted at the ISA Synchrotron Facility, University of Aarhus, Denmark, and support from the European Commission for Access to research infrastructure through the improving human potential programme.

References

[1] M. Sloth, M. Bilde, K.V. Mikkelsen, Mol. Phys. 102 (2004) 2361.
[2] N.J. Mason, A. Dawes, R. Mukerji, E.A. Drage, E. Vasekova, S.M. Webb, P. Limão-Vieira, J. Phys. B: Atom. Mol. Opt. Phys. 38 (2005) S893.
[3] A. Guenther, C.N. Hewitt, D. Erickson, R. Fall, C. Geron, T. Graedel, P. Harley, L. Klinger, M. Lerdau, W.A. McKay, T. Pierce, B. Schloes, R. Steinbrecher, R. Tallamraju, J. Taylor, P.J. Zimmerman, J. Geophys. Res. 100 (1995) 8873.
[4] J.F. Muller, J. Geophys. Res. 97 (1992) 3787.
[5] K.J. Gill, R.A. Hites, J. Phys. Chem. A 106 (2002) 2538.
[6] D. Zhang, R. Zhang, J. Chem. Phys. 122 (2005) 114308.
[7] R.J. Charlson, S.E. Schwart, J.M. Hales, R.D. Cess, J.A. Coakley, J.E. Hansen, D.J. Hoffmann, Science 255 (1992) 423.
[8] S.J. Twomey, J. Atmos. Sci. 34 (1977) 1149.
[9] B.A. Albrecht, Science 245 (1987) 1227.
[10] R.T. O'Connor, L.A. Goldblatt, Anal. Chem. 26 (1954) 1726.
[11] M.I. Al-Joboury, D.W. Turner, J. Chem. Soc. (1964) 4434.
[12] I. Novak, B. Kovac, Spectrochim. Acta A 61 (2005) 277.
[13] S. Matejcik, V. Foltin, M. Stano, J.D. Skalny, Int. J. Mass Spectrom. 9 (2003) 223.
[14] NIST Chemistry WebBook, NIST Standard Reference Database Number 69—March 2003 Release, http://webbook.nist.gov.
[15] M. Stano, S. Matejcik, J.D. Skalny, T.D. Märk, J. Phys. B: Atom. Mol. Opt. Phys. 36 (2003) 261.
[16] L.A. Curtiss, P.C. Redfern, K. Raghavachari, V. Rassolov, J.A. Pople, J. Chem. Phys. 110 (1999) 4703.
[17] Y. Zhao, J.M. Rodgers, B.J. Lynch, P.L. Fast, J. Pu, Y.-Y. Chuang, D.G. Truhlar, MULTILEVEL-Version 4.0/G03, University of Minnesota, Minneapolis, 2004.
[18] M.J. Frisch, G.W. Trucks, H.B. Schlegel, G.E. Scuseria, M.A. Robb, J.R. Cheeseman, V.G. Zakrzewski, J.A. Montgomery, R.E. Stratmann, J.C. Burant, S. Dapprich, J.M. Millam, A.D. Daniels, K.N. Kudin, M.C. Strain, O. Farkas, J. Tomasi, V. Barone, M. Cossi, R. Cammi, B. Mennucci, C. Pomelli, C. Adamo, S. Clifford, J. Ochterski, G.A. Petersson, P.Y. Ayala, Q. Cui, K. Morokuma, D.K. Malick, A.D. Rabuck, K. Raghavachari, J.B. Foresman, J. Cioslowski, J.V. Ortiz, B.B. Stefanov, G. Liu, A. Liashenko, P. Piskorz, I. Komaromi, R. Gomperts, R.L. Martin, D.J. Fox, T. Keith, M.A. Al-Laham, C.Y. Peng, A. Nanayakkara, C. Gonzalez, M. Challacombe, P.M.W. Gill, B.G. Johnson, W. Chen, M.W. Wong, J.L. Andres, M. Head-Gordon, E.S. Replogle, J.A. Pople, Gaussian 98 (Revision A.11), Gaussian, Inc., Pittsburgh, PA, 1998.
[19] R. Pariser, R.G. Parr, J. Chem. Phys. 21 (1953) 466.
[20] M. Head-Gorgon, R.J. Rico, M. Omui, T.J. Lee, Chem. Phys. Lett. 219 (1994) 21.
[21] (a) E. Runge, E.K.U. Gross, Phys. Rev. Lett. 52 (1984) 997;
(b) M.E. Casida, in: D.P. Chong (Ed.), Recent Advances in Density Functional Methods, Part I, World Scientific, Singapore, 1995, p. 155.
[22] A.A. Granovsky, PC GAMESS Version 7.1, 2008, http://classic.chem.msu.su/gran/gamess/index.html.
[23] V.A. Walter, C.M. Hadad, Y. Thiel, S.D. Colson, K.B. Wiberg, P.M. Johnson, J.B. Foresman, J. Am. Chem. Soc. 113 (1991) 4782.
[24] L.A. Curtiss, P.C. Redfern, K. Raghavachari, J.A. Pople, J. Chem. Phys. 109 (1998) 42.
[25] W. von Niessen, J. Schirmer, L.S. Cederbaum, Comput. Phys. Rep. 1 (1984) 57.
[26] P. Cecchi, A. Pizzaboica, G. Renzi, F. Grandinetti, C. Sparapani, P. Buzek, P.R. Schleyer, M. Speranza, J. Am. Chem. Soc. 115 (1993) 10338.
[27] J.P. Perdew, K. Burke, M. Ernzerhof, Phys. Rev. Lett. 78 (1997) 1396.
[28] M.E. Casida, C. Jamorski, K.C. Casida, D.R. Salahub, J. Chem. Phys. 108 (1998) 4439.
[29] D.J. Tozer, N.C. Handy, J. Chem. Phys. 109 (1998) 10180.
[30] S. Eden, P. Limão-Vieira, S.V. Hoffmann, N.J. Mason, Chem. Phys. 323 (2006) 313.